COMPUTATIONAL PATHOLOGY: THE THIRD PATHOLOGY'S REVOLUTION CAN BE APPLIED TO CRC SCREENING?

Prof. Paola Cassoni

Pathology Unit, Dept. Medical Sciences

University of Turin, Italy

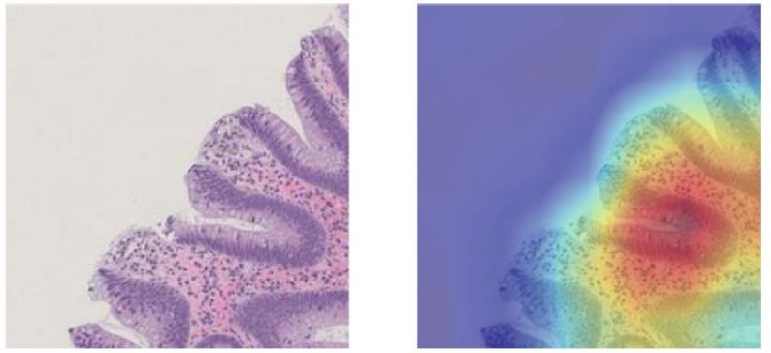

(b) HP

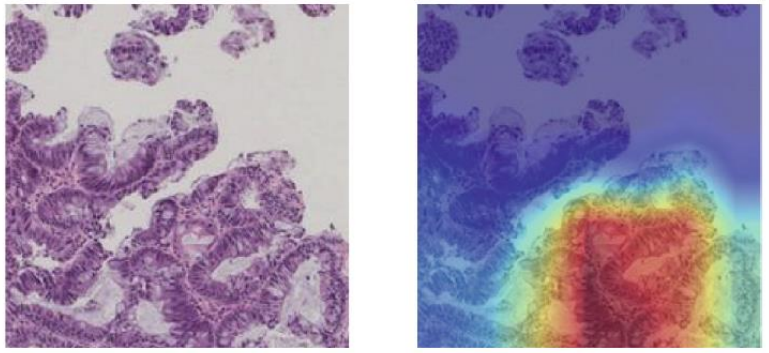

(d) HG

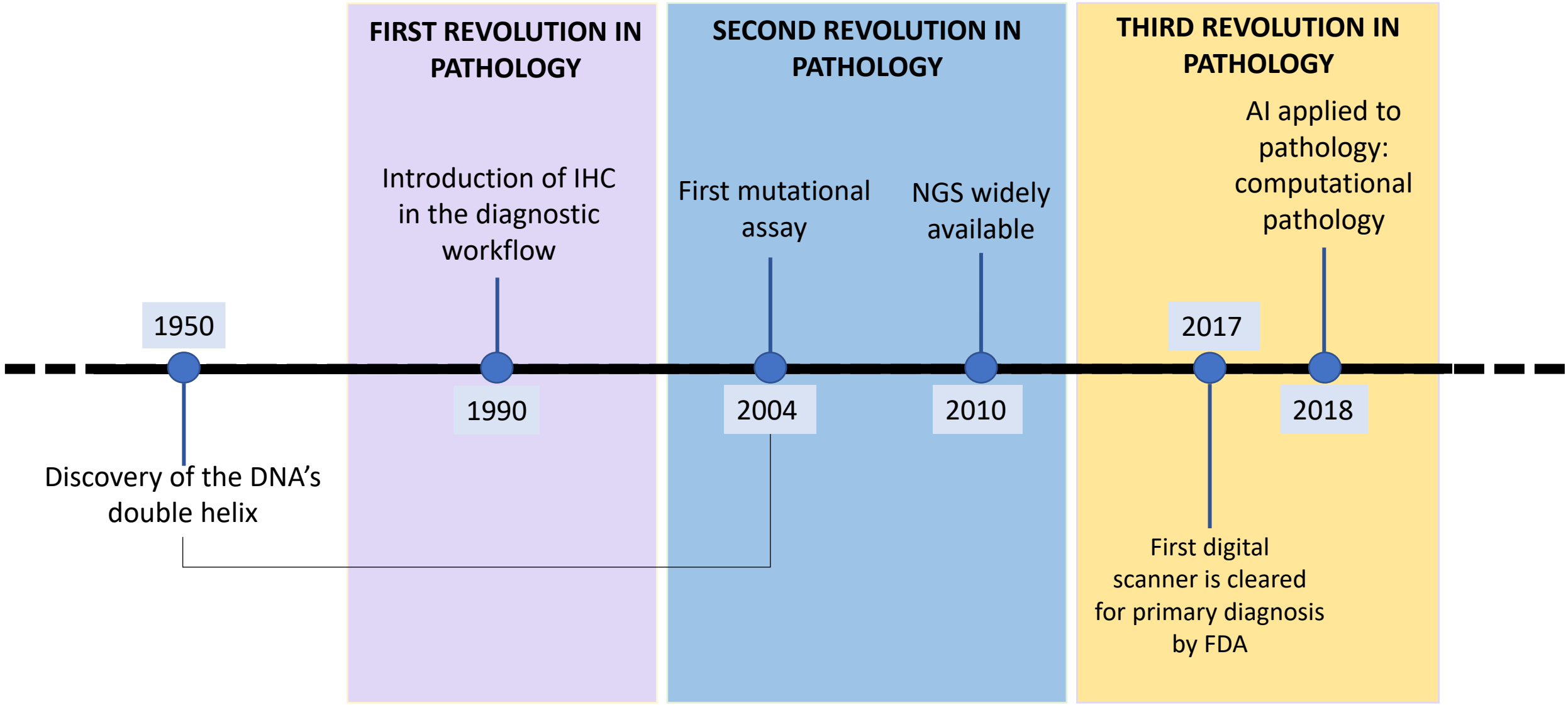

Adapted from Shafi, S., Parwani, A.V. *Diagn Pathol* (2023)

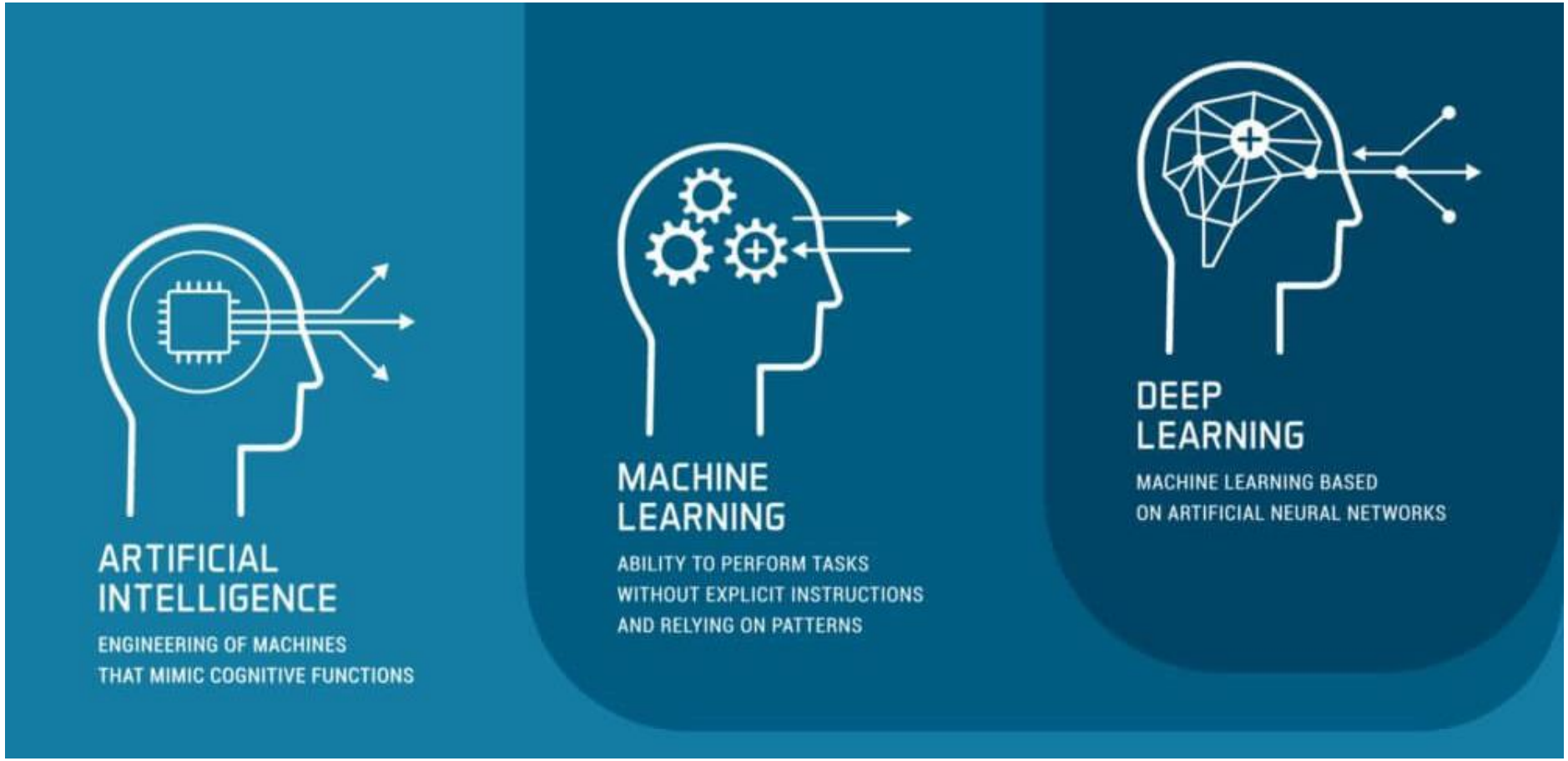

- Explicit programmig
- Predetermined features selection
- Multiple interactions pathologists/informaticians needed
- Time consuming

- Automated learning
- Freely available source codes of effective neural network architectures
- Superior results in most cases

COMPUTATIONAL PATHOLOGY "WORKFLOW"

Digital pathology
The digitization of the traditional diagnostic process of analyzing cells and tissue with a microscope via whole-slide scanners and computer screens.

Whole-slide images
Digital images obtained by digitizing complete histopathological glass slides using a high-resolution scanner.

Image segmentation
The operation of decomposing the semantic content of an image into multiple segments, where each segment contains pixels belonging to the same semantic category (for example, the tumor region).

Model regularization
In machine learning, indicates the process of constraining a model's parameters to small values, discouraging complex models, therefore reducing the risk of overfitting the training data.

Training

Application

Computational pathology
The computational analysis of digital images obtained through scanning slides of cells and tissues.

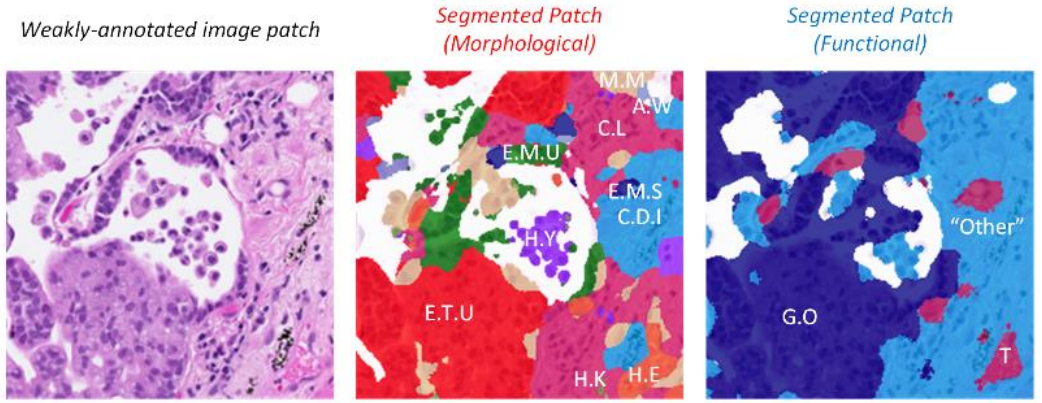

Patch-level annotations

- Exocrine Gland (G.O)
- Transport Vessel (T)
- Stratified Cuboidal Epithelium (E.T.U)
- Simple Cuboidal
- Epithelium (E.M.U)
- Leukocytes (H.K)
- Lymphocytes (H.Y)
- Loose Connective (C.L)
- Smooth Muscle (M.M)
- White Adipose (A.W)
- Erythrocytes (H.E)
- Simple Squamous Epithelium (E.M.S)

Mitosis detection

Cell detection & counting

IHC evaluation

Tumor detection, classification and grading

DIAGNOSTIC PURPOSE

PROGNOSTIC PURPOSE

Van der Laak et al. *Nat Med* (2021)
Chan L. et al., *ICCV* (2019)

- Predetermined feature selection
- Multiple interactions pathologists/informaticians needed
- Time consuming

Feature engineering

Deep learning

- Automated learning
- Freely available source codes of effective neural network architectures
- Superior results in most cases

Deep learning overall workflow:

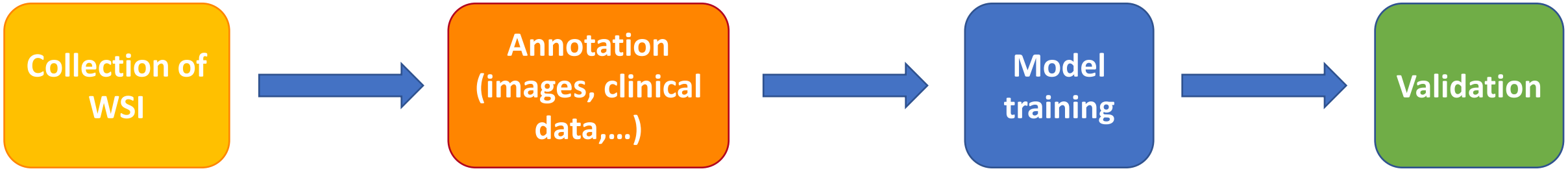

Digital pathology for colorectal carcinoma

- Distinction between tumor tissue and stroma (Kather JN et al. *Sci Rep* 2016)
- Outcome prediction (Bychkov D et al. *Sci Rep* 2018; Kather JN et al. *PLoS Med* 2019; Skrede O et al. *Lancet* 2020)
- Molecular profile prediction (Yamashita R et al., *Lancet Oncol* 2020; Sirinukunwattana K et al. *Gut* 2021; Bilal M et al. *Lancet Digit Health* 2021)

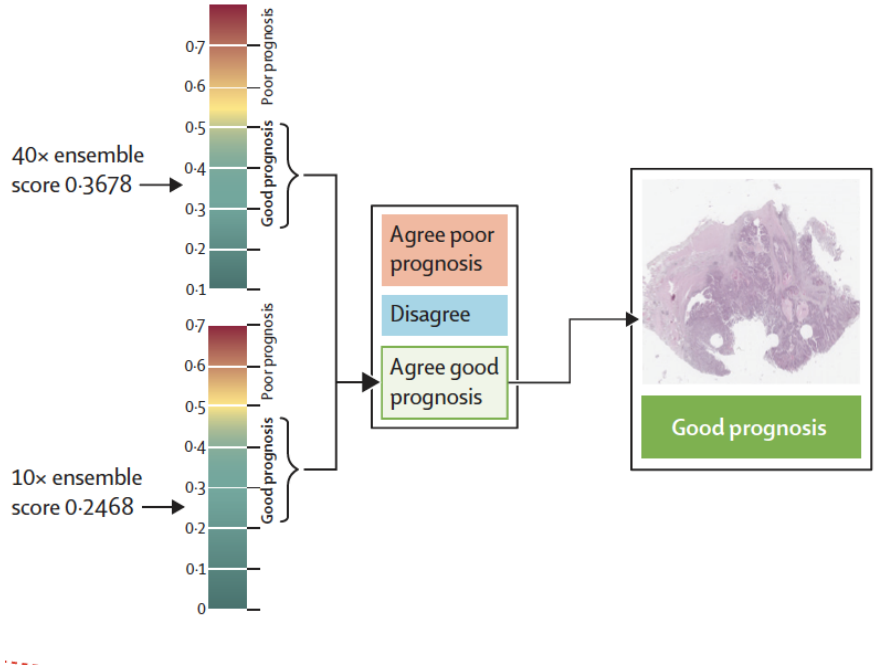

- Adenoma classification…

Adenoma classification

JAMA Network Open

Original Investigation | Health Informatics

Evaluation of a Deep Neural Network for Automated Classification of Colorectal Polyps on Histopathologic Slides

Jason W. Wei, BA; Arief A. Suriawinata, MD; Louis J. Vaickus, MD, PhD; Bing Ren, MD, PhD; Xiaoying Liu, MD; Mikhail Lisovsky, MD, PhD; Naofumi Tomita, MS; Behnaz Abdollahi, PhD; Adam S. Kim, MD; Dale C. Snover, MD; John A. Baron, MD; Elizabeth L. Barry, PhD; Saeed Hassanpour, PhD

JAMA Network Open. 2020;3(4):e203398. doi:10.1001/jamanetworkopen.2020.3398

Figure 1. Data Flow Diagram for the Study

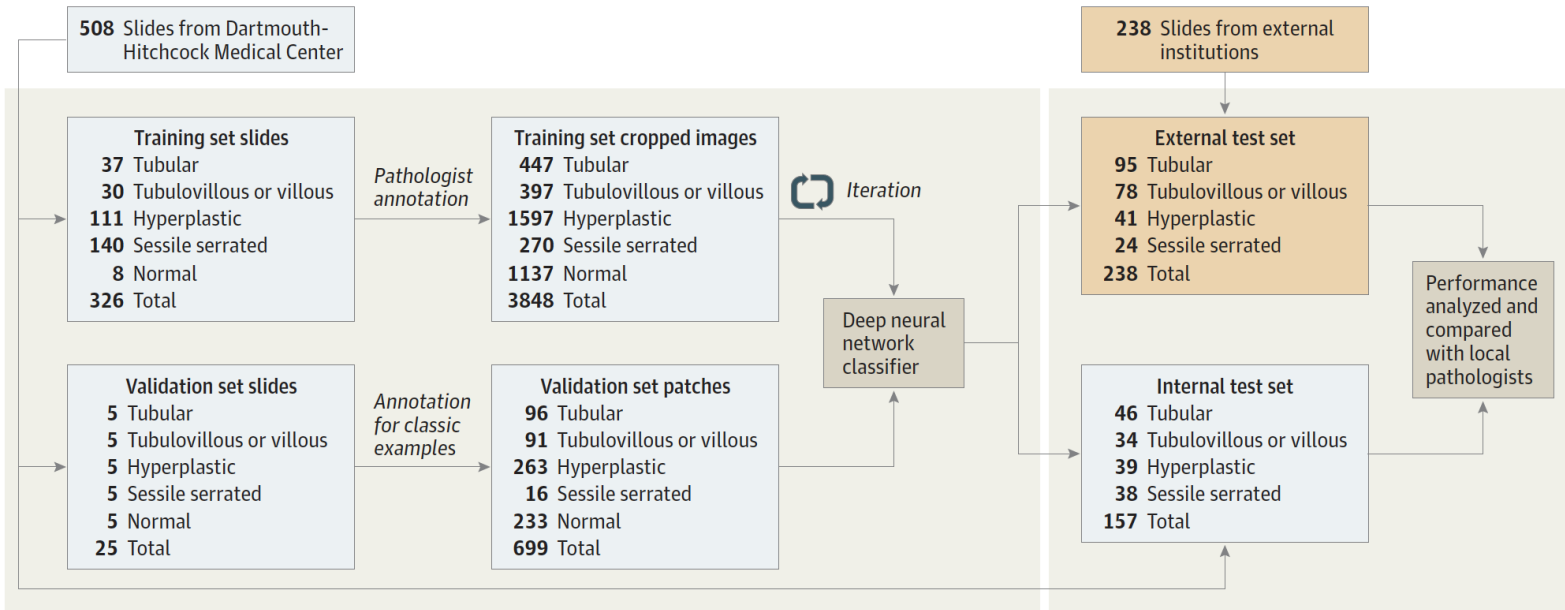

Adenoma classification

Table. Per-Class Comparison Between Local Pathologists and the Deep Neural Network Model in Classifying Colorectal Polyps on Internal and External Test Sets

	Internal test set (n = 157)						External test set (n = 238)					
	Local pathologists			Deep neural network			Local pathologists			Deep neural network		
Polyp type	Accuracy, %	Sensitivity, %	Specificity, %	Accuracy, %	Sensitivity, %	Specificity, %	Accuracy, %	Sensitivity, %	Specificity, %	Accuracy, %	Sensitivity, %	Specificity, %
TA	89.8	76.1	95.5	93.0	89.1	94.6	79.8	53.7	97.2	84.5	73.7	91.6
TVA	94.3	88.2	95.8	95.5	97.1	95.1	81.5	100	77.7	89.5	97.6	87.8
HP	89.8	76.9	94.1	92.4	82.1	95.8	91.6	80.8	96.8	85.3	60.3	97.5
SSA	91.7	81.6	95.0	93.0	78.9	97.5	93.3	79.2	94.8	88.7	79.2	89.7
Mean	91.4	80.7	95.1	93.5	86.8	95.7	86.6	78.4	91.6	87.0	77.7	91.6

Limitations:

- **Lack of dysplasia grading**
- Lack of normal tissue
- Lower performance during external testing

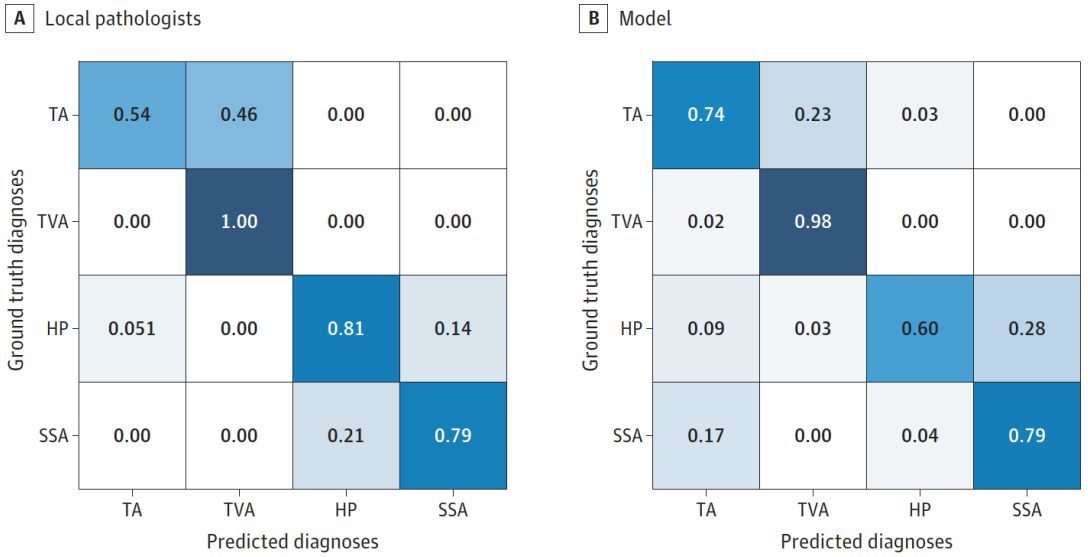

JAMA Network Open. 2020;3(4):e203398. doi:10.1001/jamanetworkopen.2020.3398

High Performance Computing boosting Biomedical Applications

DEEPHEALTH

PARTNERS

22 partners from 9 European Countries

Research Organisations

Universitat Politècnica de València
Università degli Studi di Torino
Barcelona Supercomputing Center – Centro Nacional de Supercomputación
list
UNIMORE – Università degli Studi di Modena e Reggio Emilia
CRS4
Otto von Guericke Universität Magdeburg
EPFL
Karolinska Institutet
security tech Stelar law research

Health Organisations

Azienda Ospedaliero-Universitaria Città della Salute e della Scienza di Torino
CHUV
Fundación para el Fomento de la Investigación Sanitaria y Biomédica de la Comunitat Valenciana
Spitalul Clinic Prof. Dr. Theodor Burghele București
Stockholms läns landsting

Large Industrial Partners

SIMAVI – Software Imagination & Vision
everis – an NTT DATA Company
PHILIPS
THALES

SME Industrial Partners

WINGS ICT Solutions
prodesign electronic gmbh
TREE Technology

Aim

Provide **High Performance Computing (HPC)** power at the service of biomedical applications; and apply **Deep Learning** (DL) and **Computer Vision** (CV) techniques on large and complex biomedical datasets to support new and more efficient ways of diagnosis, monitoring and treatment of diseases

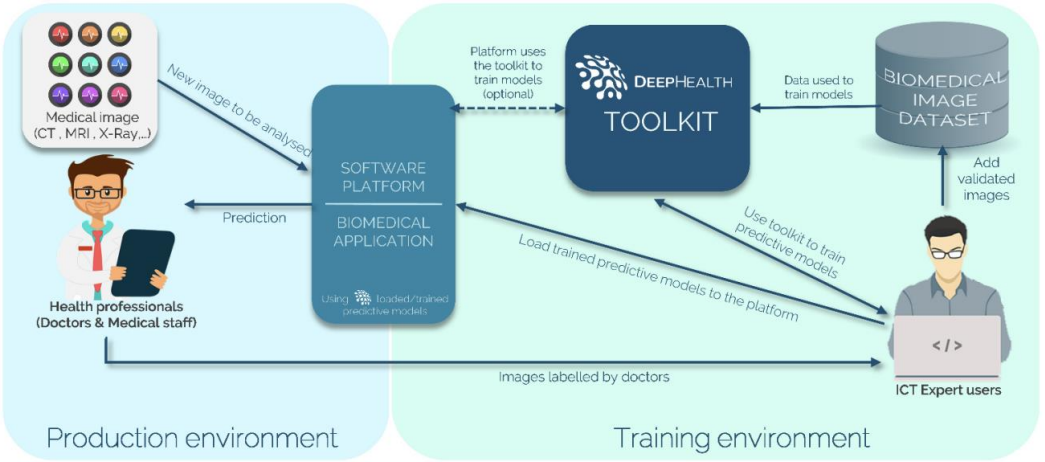

This project has received funding from the European Union's Horizon 2020 research innovation programme under grant agreement No. 825111

DEEPHEALTH

UNIVERSITÀ DEGLI STUDI DI TORINO

UniTOPatho

DIPARTIMENTO di SCIENZE MEDICHE unito.it

di.unito.it DIPARTIMENTO DI INFORMATICA

Use Cases

14 pilot test-beds in 3 areas:

Neurological diseases

- Migraine and Seizures prediction
- Major Depression
- Dementia
- Study of structural changes in lumbar spine pathology
- Population model for Alzheimer's Disease
- Epileptic seizures detection
- Objective fatigue assessment for multiple sclerosis patients

Tumor detection and early cancer prediction

- Chest cancer detection
- Prostate tumor diagnosis
- Skin cancer melanoma detection

Digital pathology and automated image annotation

- Classification of whole-slide histological images of colorectal biopsy samples
- CT brain perfusion maps synthesis
- Deep Image annotation
- Image Analysis and prediction for Urology

Colon cancer diagnosis

DeepHealth

Colon cancer is one of the most frequent causes of death. Screening programs can enable prompt diagnosis and treatment of this aggressive disease, but they also lead to higher caseloads and costs for the already strained European healthcare services. DeepHealth can help streamline pathological diagnosis of colon biopsies.

Dataset (WSI images)

	HP	NORM	TA.HG	TA.LG	TVA.HG	TVA.LG	Total
Slides	62	30	34	232	44	55	**457**
R_t	158	112	145	777	264	245	**1701**
A_t $[\mathrm{cm}^2]$	9.91	18.38	7.94	71.74	60.45	41.86	**210.29**

- H&E slide acquired on the Hamamatsu Nanozoomer S210 scanner (200X)

- Manual annotation according to 6 classes:

  - NORM: normal tissue
  - HP: hyperplastic polyp
  - TA.LG: tubular adenoma, low-grade dysplasia
  - TA.HG: tubular adenoma, high-grade dyplasia
  - TVA.LG: tubulo-villous adenoma, low-grade dysplasia
  - TVA.HG: tubulo-villous adenoma, high-grade dysplasia

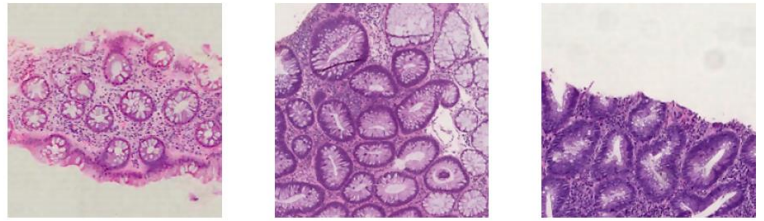

(a) NORM (b) TA.LG (c) TA.HG

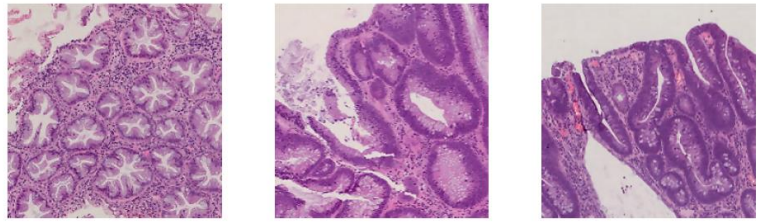

(d) HP (e) TVA.LG (f) TVA.HG

Perlo D. et al. MICAD 2021

Dysplasia grading

Table 4. WSI inferences: confusion matrices.

(a) φ =600 µm, gray-scale

Gr. truth \ Predicted	HP	NORM	HG	LG
HP	**0.85**	0	0.05	0.1
NORM	0.12	**0.75**	0	0.12
HG	0.02	0	**0.63**	0.35
LG	0.03	0.09	0.18	**0.7**

(b) φ =600 µm, RGB

Gr. truth \ Predicted	HP	NORM	HG	LG
HP	**0.75**	0.05	0	0.2
NORM	0	**0.62**	0	0.38
HG	0	0.02	**0.61**	0.37
LG	0.03	0.06	0.15	**0.76**

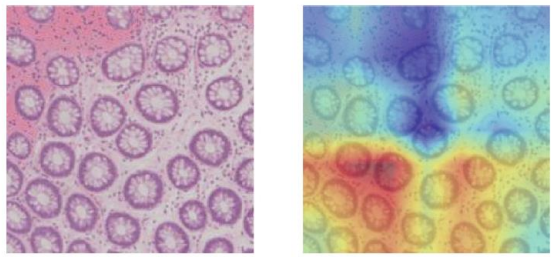

(a) NORM

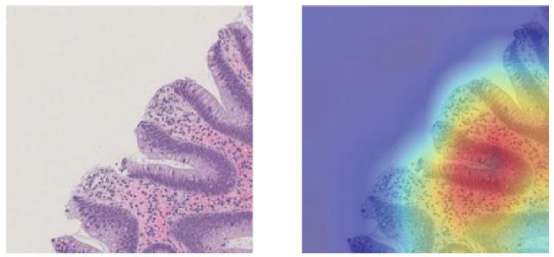

(b) HP

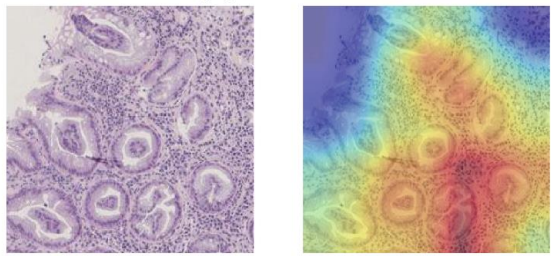

(c) LG

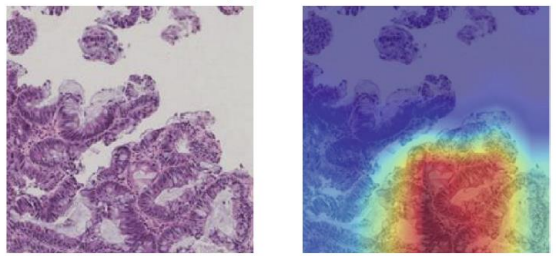

(d) HG

- Poor results in distinguishing TA versus TVA/VA

Perlo D et al. MICAD 2021

Multi-resolution analysis

	Patch scale σ [µm]					
Type	100	800	1500	4000	7000	8000
BA (6-class)	0.40	0.45	**0.46**	0.41	0.37	0.38
NORM	0.70	0.66	0.72	0.76	0.78	0.71
HP	0.81	**0.92**	0.85	0.70	0.60	0.69
TA (HG+LG)	0.65	0.66	0.65	0.71	**0.76**	0.70
TVA (HG+LG)	0.64	0.67	0.68	0.74	**0.84**	0.76

Table 2: Preliminary experiments: overall BA for all of the six classes (first row) and BA for each polyp type, plus normal tissue.

- Adenoma type and dysplasia grade are best classified at different scales

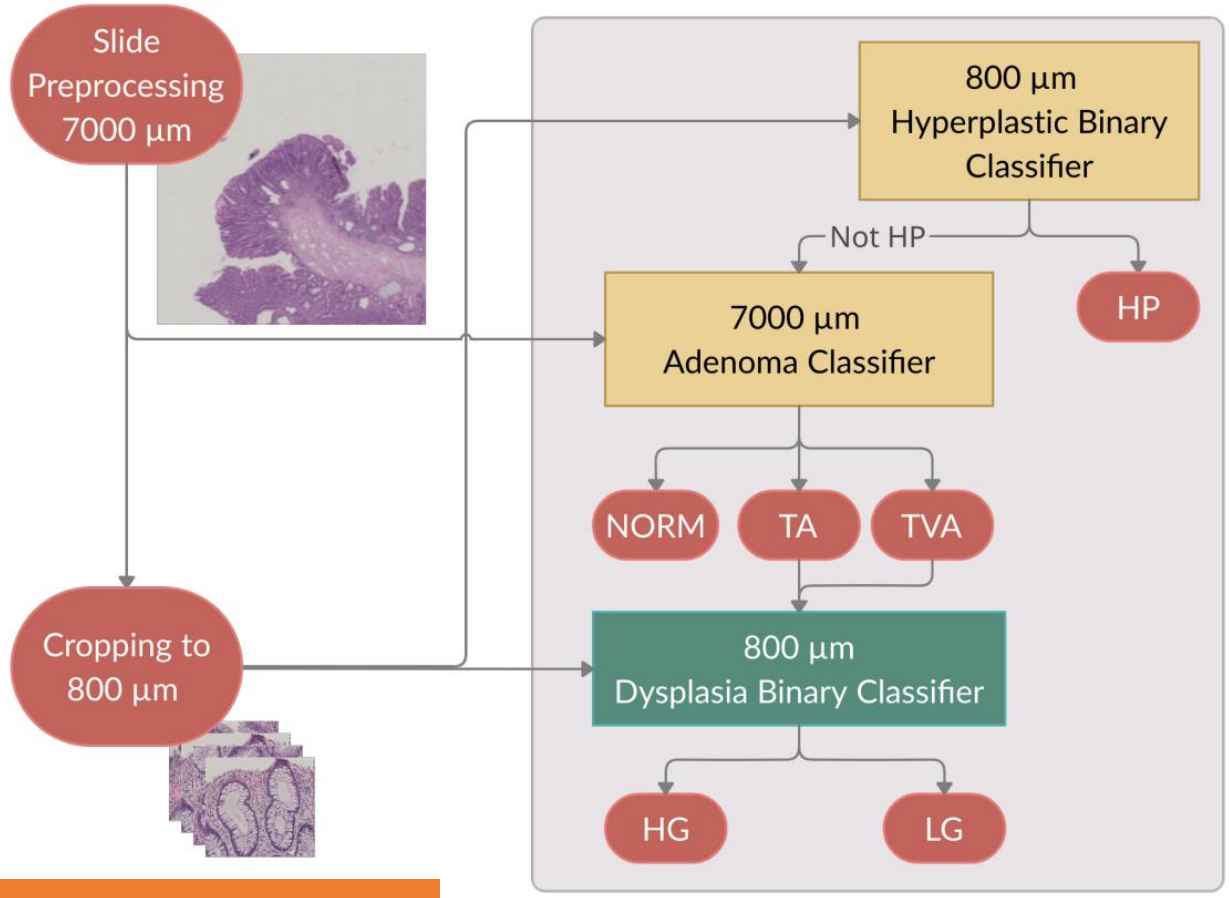

Limitations:

- **Some entities missing (serrated adenomas, invasive adenocarcinomas,…)**
- **Larger dataset is warranted**
- **Lack of external validation**

Barbano CA et al. IEEE ICIP 2021

OPEN

A promising deep learning-assistive algorithm for histopathological screening of colorectal cancer

SCIENTIFIC REPORTS, 2023
nature portfolio

Cowan Ho[1,6], Zitong Zhao[2,6], Xiu Fen Chen[2,6], Jan Sauer[3], Sahil Ajit Saraf[3], Rajasa Jialdasani[3], Kaveh Taghipour[3], Aneesh Sathe[3], Li-Yan Khor[2,4], Kiat-Hon Lim[2,4] & Wei-Qiang Leow[2,4,5]✉

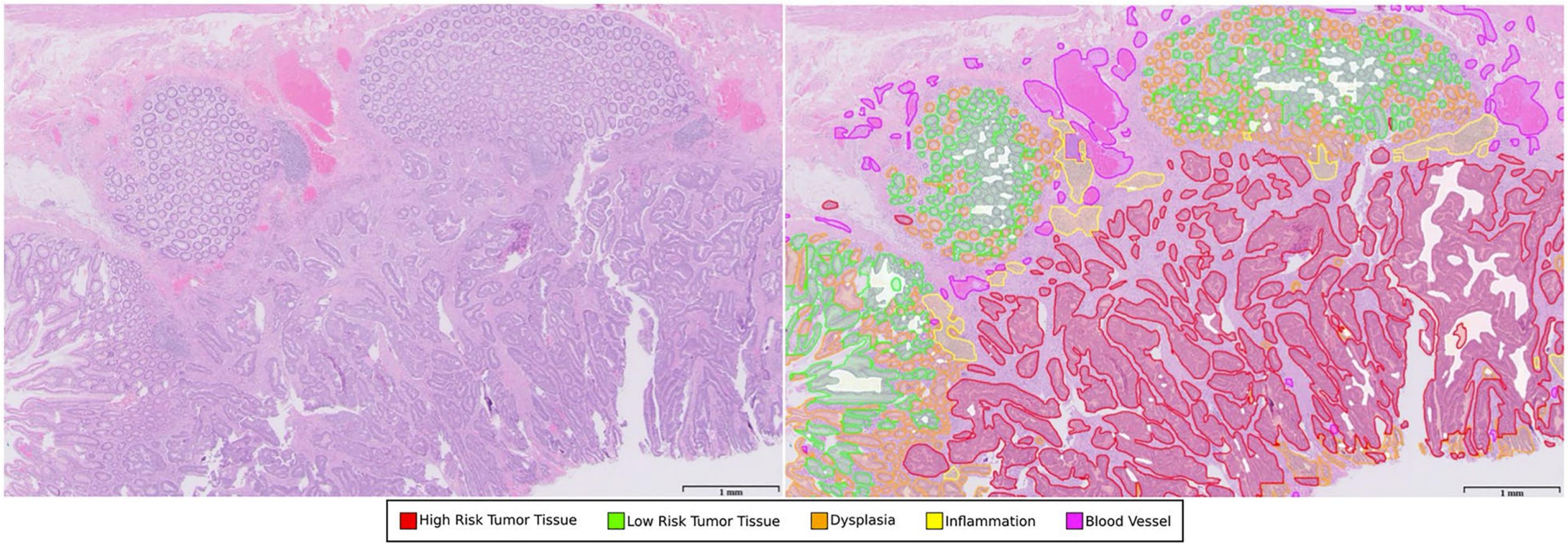

Figure 1. A sample analysis on a whole slide image (WSI). Left: original image. Right: the segmentation model highlighted regions of the WSI as (1) likely benign or normal (green), (2) likely dysplastic (orange), and (3) likely malignant (red). The AI model also segmented blood vessels (pink) and inflammation (yellow), and these segmentations were taken into account for slide labeling.

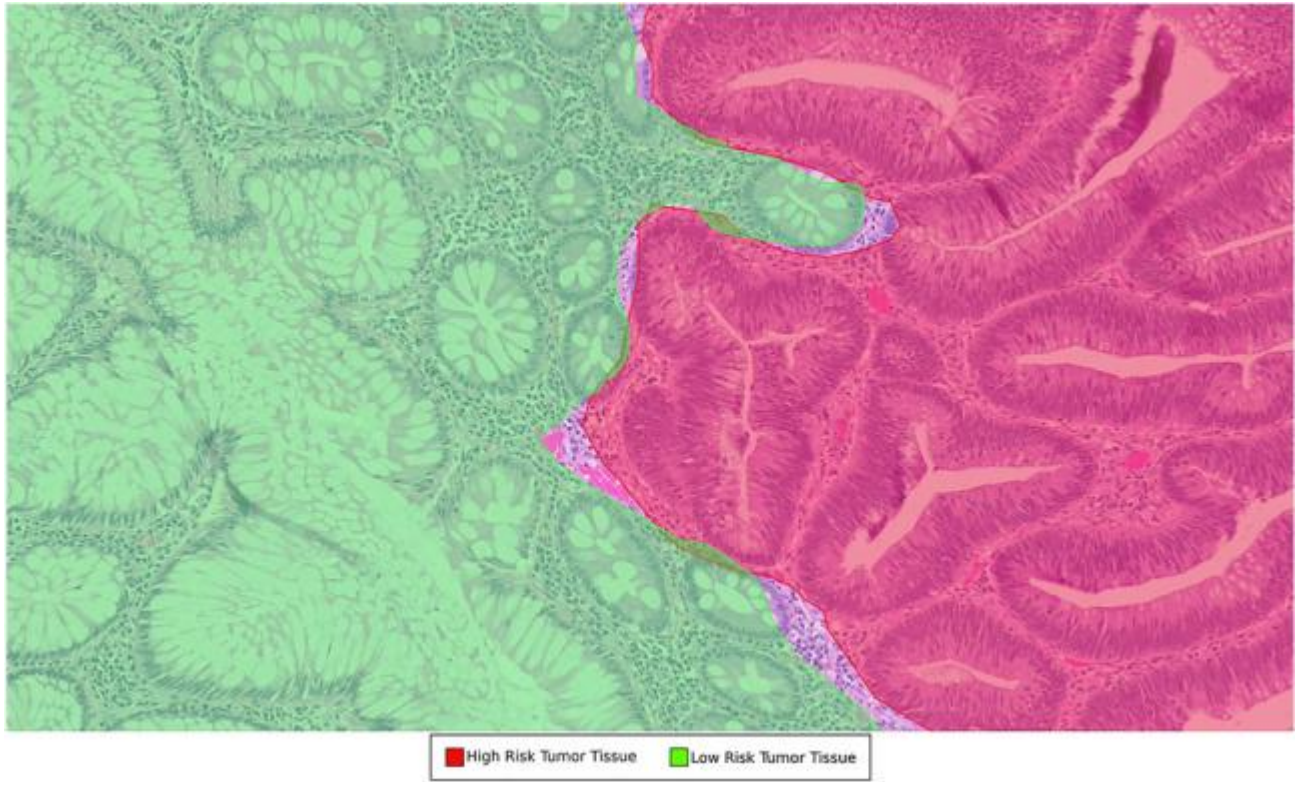

Biopsies		Ground Truth	
		High Risk	Low Risk
Prediction	High Risk	TP: 75	FP: 29
	Low Risk	FN: 2	TN: 44

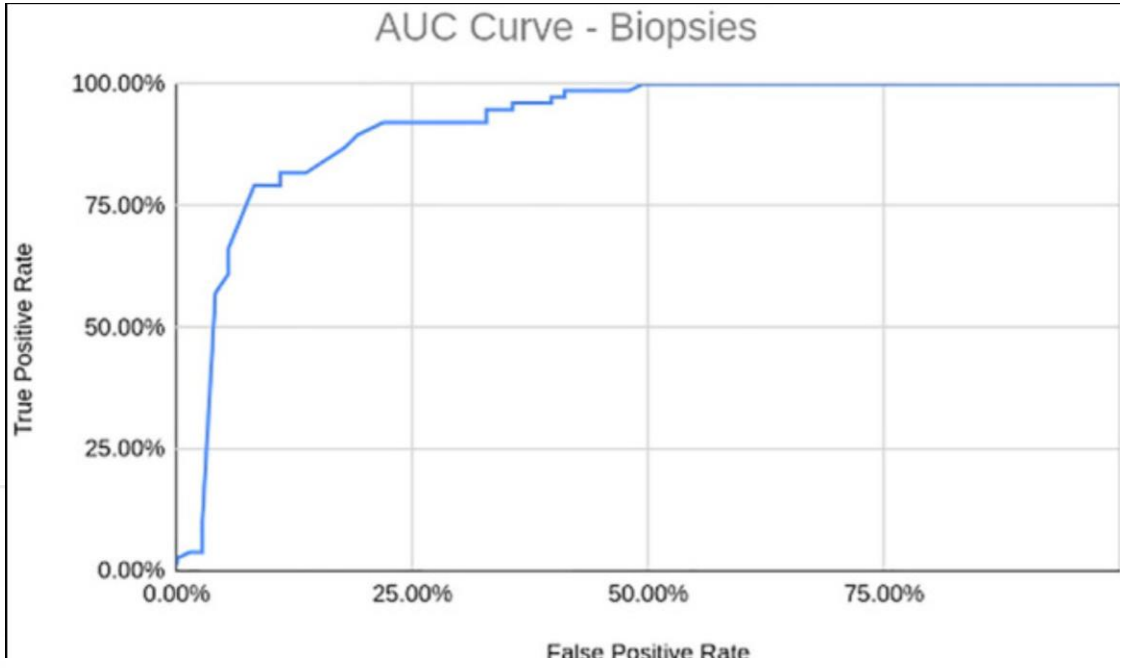

Figure 4 AUC curve from applying the AI model on the validation set of 150 WSIs. The system achieves an AUC of 91.7%.

CONCLUSIONS

Upon evaluation of the output data from the validation set, its high AUC of 91.7 demonstrates a good concordance between the AI model and the expert pathologist. With a sensitivity of 97.4, it validates our AI model to function as a screening tool that minimizes false negatives extensively. This favour of sensitivity over specificity shows its usability in assistive workflow and has added practicality into the application of a clinical workflow. Since our AI model is designed solely as an assistive tool, the final diagnosis during reporting remains with the pathologist. This high sensitivity ensures with greater certainty that all lesions suspicious for malignancy are h
diagnostic workf
other possible w
act as first reade

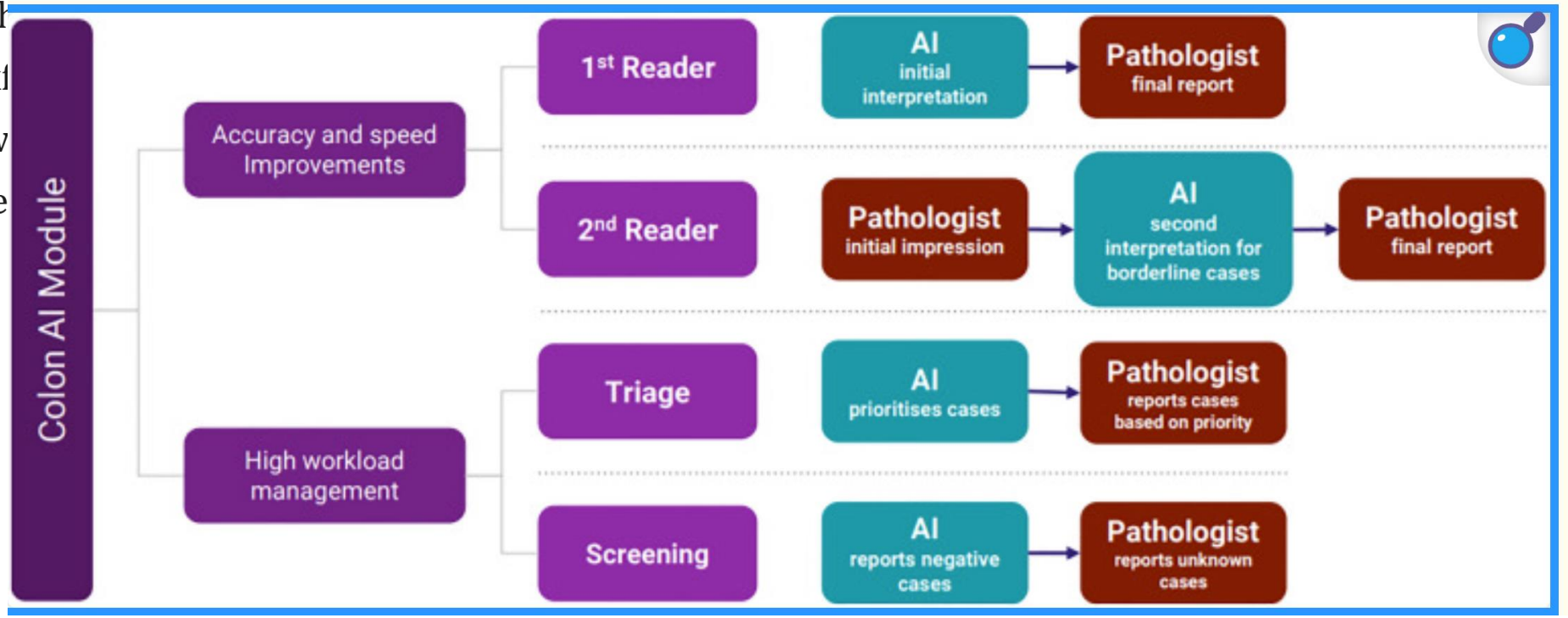

To sum up:

CPATH is the third revolution in pathology and when applied CRC SCREENING may helps to **identify** and **distinguish benign and cancerous glands, as well as low and high dysplasia**→ implementing these technoloy in the diagnostic workflow would result in a ***reduction*** of turn around time, workload, misdiagnosis and lab costs however some challenges are still open.

FUTURE PERSPECTIVES ON CPATH

- Implement novel tool to minimize errors
- Improve the pathology units worldwide (e.g. slide scanner, IT unit ecc…)
- Train pathologists to use WSI and CPATH

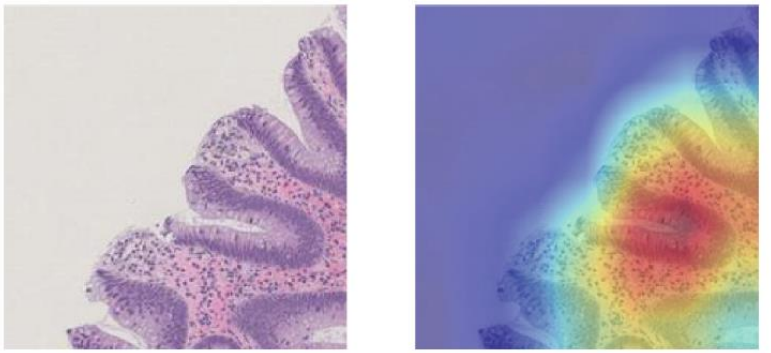

(b) HP

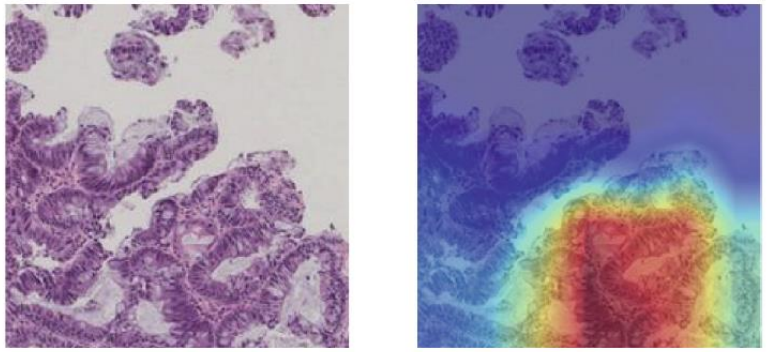

(d) HG